Towards Synthetic Vascular Graft Monitoring Using a Flip-Chip-on-Flex Impedance Spectroscopy Sensor

IEEE Sensors Council

Towards Synthetic Vascular Graft Monitoring Using a Flip-Chip-on-Flex Impedance Spectroscopy Sensor

Jamie R. K. Marland, Andreas Tsiamis, Daniel Hoare, Pablo G. Ledesma Lopez, Steven L. Neale, John R. Mercer & Srinjoy Mitra

***Abstract* — Synthetic vascular grafts are used in a wide range of clinical applications. However, they can become prone to occlusion over time, due to growth of vascular smooth muscle cells (VSMC). This phenomenon is associated with graft failure. Here, we describe novel techniques for packaging and integration of a miniature sensor of VSMC growth. The sensor was based on a microfabricated array of interdigitated platinum electrodes on a silicon substrate. It was assembled using flip-chip-on-flex technology to create a low-profile package that can be manufactured using industry-standard tools and is suitable for integration with a synthetic vascular graft. The packaged sensor responded to changes in solution impedance, and accurately detected growth of VSMC in vitro. We also demonstrated successful proof-of-concept integration of the sensor with a custom synthetic graft. Together these technologies have the potential to allow early detection of VSMC growth prior to graft occlusion, enabling more timely and effective clinical interventions to be made.**

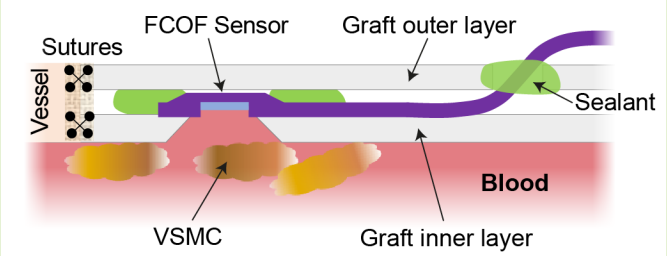

***Index Terms* — Implantable medical device, synthetic vascular graft, impedance sensor, vascular smooth muscle cells, impedance spectroscopy, microfabrication, flip-chip-on-flex packaging**

I. Introduction

SYNTHETIC vascular grafts are artificial tubes designed to replace or augment existing blood vessels. These implantable devices are commonly used to create arteriovenous (AV) access points in patients receiving haemodialysis [1]. However, a major problem with synthetic grafts is occlusion (blockage) of the lumen, which reduces their effectiveness and can result in graft failure. For example, synthetic haemodialysis AV access points perform poorly: one year after implantation, standard expanded polytetrafluoroethylene (ePTFE) grafts have a patency rate (functionality) of only 57% [2].

Early detection of implant failure, before complete occlusion and thrombosis occurs, allows for simpler interventions to be used to improve flow or prevent worsening. This leads to improved patient outcomes. However, clinical assessment alone can miss the early signs of failure, and occlusion may occur between examinations [3]. A mechanism for continuous implant monitoring would therefore improve early detection of failures. Blood pressure and flow sensing devices have previously been described for monitoring graft condition, and they can potentially detect an occlusion once it has become established [4]-[7]. However, the earlier root cause of occlusion in synthetic grafts is typically neointimal hyperplasia – the excessive growth of vascular smooth muscle cells (VSMC) – particularly at the anastomosis (join) between the graft and native vessels (Fig. 1a,b) [8]. A mechanism to detect the VSMC growth at this early stage, before flow disruption has occurred, would therefore offer a significant clinical advantage.

To meet this need, we propose sensors integrated within synthetic grafts that use electrical impedance spectroscopy (EIS) to detect VSMC growth. In this study we focus on synthetic AV grafts, but the technology could equally be applied to other synthetic graft applications such as aneurysm and bypass surgery, and to vascular stents, where impedance sensing has already been shown be effective [9]-[12].

EIS sensor systems for characterising cell growth have a long history and are well understood [13]. They typically consist of an interdigitated electrode (IDE) array coupled to impedance measurement instrumentation and sense the presence of cells and their characteristics through changes in the complex impedance between the electrodes [14]. To accommodate an IDE sensor within a synthetic vascular graft, the sensors must

Manuscript submitted for review April 8th, 2022. This work was supported by the MRC Confidence in Concept Scheme at the University of Edinburgh (MRC/CIC6/63) and University of Glasgow; EPSRC (EP/S515401/1, EP/R020892/1); and the UK Chief Scientist Office (CGA/17/29). For the purpose of open access, the author has applied a Creative Commons Attribution (CC BY) licence to any Author Accepted Manuscript version arising from this submission.

J. R. K. Marland, A. Tsiamis, P. G. Ledesma Lopez, and S. Mitra are with School of Engineering, Institute for Integrated Micro and Nano Systems, University of Edinburgh, Edinburgh, EH9 3FF, UK (e-mail: jamie.marland@ed.ac.uk).

S. L. Neale is with the Centre for Medical and Industrial Ultrasonics, James Watt School of Engineering, University of Glasgow, Glasgow, G12 8QQ, UK.

D. Hoare and J. R. Mercer are with the Institute of Cardiovascular and Medical Sciences/British Heart Foundation, University of Glasgow, Glasgow, G12 8TA, UK.

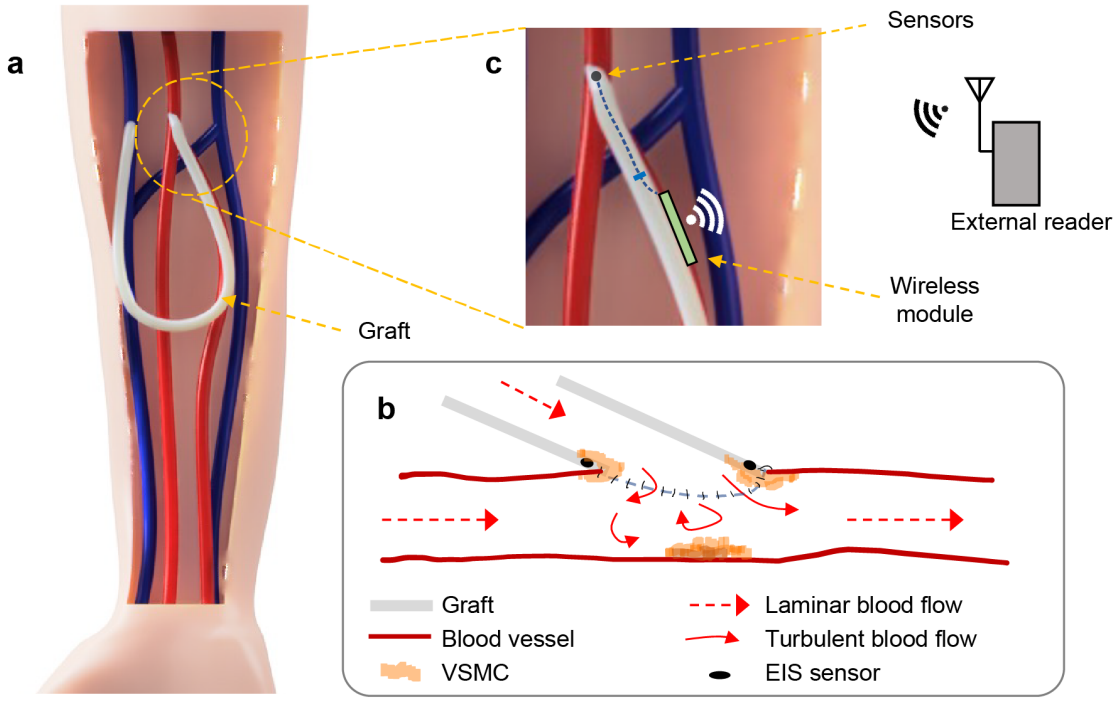

Fig. 1. Vascular graft stenosis and reporting. (a) Placement of a synthetic AV graft in the human forearm act as a shunt between an artery and vein, providing a resealable surface area for repeated canulation. (b) VSMC growth at the sutured graft-vessel boundary termed anastomosis. (c) Possible position of a miniature implanted sensor that can be monitored using subcutaneous wireless transmitters.

be sufficiently miniaturised and offer the possibility of accommodating circuits for front-end electronics, digitization, and wireless communications.

An ideal sensing device would be positioned entirely within the desired location of graft-vessel boundary and completely encapsulated by the graft. However, such a tiny implant system would be challenging to produce, primarily due to the physical limitation of the wireless antenna size necessary to communicate with an external reader. An alternative solution is placement of the EIS transducer (along with necessary electronics) within the graft, and connection to a separate wireless device situated outside the graft (Fig. 1c). Various graft applications where the target vessels are close to the skin surface would be easily accessible in this way.

Silicon-based EIS sensors are ideal in this application, offering several advantages. They would: (1) enable direct integration of a sensor and associated CMOS readout electronics, resulting in the smallest form factor and improved readout quality by reducing interconnect distances; (2) minimise cost of the complete sensor, since CMOS devices are inexpensive when manufactured in volume; and (3) enable very consistent performance, essential for both clinical utility and regulatory approval, due to the tight process control used during semiconductor manufacturing. Such sensors can be manufactured using established techniques for post-processing CMOS devices with additional electrode materials, either at die level [15] or wafer level [16].

However, silicon-based sensors are challenging to integrate with implantable devices. In their traditional usage, silicon-based devices are connected via bond pads to the external world, while the core of the device is protected by passivation layers. In contrast, implanted sensors often have a sensing area within their core that must be exposed to directly access the environment, while the bond pads must be well protected to avoid corrosion. The ubiquity of silicon devices in other application areas has led to development of advanced assembly and packaging methods that can be adapted and applied in novel ways to meet the conflicting needs of implanted silicon sensors. Here, we applied flip-chip die bonding on a flexible substrate ("flip-chip-on-flex", FCOF) as a solution. Development of FCOF technology has been driven by applications in which a small form-factor and an ability of the substrate to bend and conform to other structures are important, such as in wearable devices. We believe that they may also be useful in the manufacture of implantable devices.

Compared to traditional wire bonding, flip-chip bonds are more robust and scalable, and they also reduce the volume of the integrated device – highly desirable in this application. Flip-chip bonding also involves mounting the die face-down, enabling the substrate to become part of the package design. We took advantage of this feature to add a window in the substrate beneath the die, selectively exposing its sensing elements to the environment. This avoids the requirement for complex encapsulation patterning techniques that we have previously needed for wire-bonded (face-up) implantable sensors [17]. In a typical rigid flip-chip assembly process, metallic bumps are applied to the die, followed by die alignment and bonding to the substrate pads, and finally application of an underfill to insulate and support the bonds [18]. In FCOF assembly, non-conductive or anisotropic conductive adhesives can be used to form the bonds [19], however we opted to retain conventional gold stud bumping and thermosonic bonding to maximise bond strength [20]. In this study, we report the fabrication, assembly, and packaging of a complete FCOF impedance sensor for graft applications.

II. Materials & Methods

A. Sensor die microfabrication

IDE devices were fabricated on 100 mm diameter, n-type, <100> orientation, silicon wafers (Si-Mat), using standard processes that are in widespread use for industrial integrated circuit manufacturing. The wafer was first thermally oxidised to create a bottom insulator layer of 500 nm silicon dioxide. Electrodes and fiducials (optical alignment marks) were then fabricated from a layer of 50 nm platinum (with an underlying adhesion layer of 10 nm titanium) that was deposited by e-beam evaporation and patterned using a photoresist lift-off process. Bond pads and interconnect were fabricated from a layer of 1000 nm aluminium that was deposited by sputtering and patterned using a photoresist lift-off process. A top insulator layer of 1000 nm silicon nitride was deposited using plasma-enhanced chemical vapour deposition, then patterned using photolithography and reactive ion etching in a CF_4/O_2 plasma to expose the electrode and bond pad areas. During these processing steps, care was taken to minimise duration of exposure to water to prevent galvanic corrosion of the aluminium features. Finally, a layer of protective photoresist was deposited on the wafer, and it was diced into 1.40 mm × 3.00 mm dies. The protective photoresist layer was stripped off prior to packaging.

B. Flexible substrate manufacture

The substrate was manufactured by Merlin Flex Ltd (UK) as a flexible polyimide printed circuit board design. It consisted of a 50 μm thick base layer (25 μm polyimide and 25 μm adhesive) with 35 μm thick copper tracks, a top layer of 50 μm thick coverlay (25 μm polyimide and 25 μm adhesive), and a bottom stiffener layer (250 μm polyimide). All exposed copper was ENIG (electroless nickel immersion gold) coated.

C. Assembly and packaging

Basic assembly of the sensor on the flex was performed in collaboration with Alter Technology (UK). The die bond pads were first prepared by bumping with gold stud bumps. The die was then attached to the flexible substrate using a flip-chip bonding process. Specifically, the flexible substrate was held in a custom jig and the die held in a custom pickup tool (designed for die dimensions of 1350 μm × 2950 μm), then the substrate and die were optically aligned using their corner fiducials and attached by thermosonic bonding using a Finetech Fineplacer tool. To mechanically support and electrically insulate the bonds, a layer of OP21G urethane acrylate underfill (Dymax) was applied between the die and substrate, and cured by UV exposure. Bonds were inspected using micro-focus radiography. Finally, a ring of EPO-TEK OG116-31 biocompatible epoxy (Epoxy Technology Europe Ltd.) was deposited around the die edges and exposed substrate interconnect to provide complete insulation. The epoxy was cured by UV exposure, and its biocompatibility and moisture resistance were ensured by baking at 80˚C for 120 min and 150˚C for 5 min.

D. Electrochemical measurements

Integrated FCOF sensors were initially characterised in solution using an Autolab PGSTAT12 potentiostat equipped with a FRA2 impedance module (Metrohm AG) and controlled by NOVA 1 software (Metrohm AG). The packaged sensor under test was attached to the potentiostat via a miniature flat flexible cable (FFC) connector, with one IDE electrode connected to shorted working/sense electrode leads, and the other IDE electrode connected to shorted counter/reference electrode leads. Impedance was measured in either air, de-ionised water, or phosphate buffered saline (PBS) containing 154 mM NaCl and 10 mM phosphate buffer at pH 7.4. Measurements were made using a 10 mV amplitude test signal, sweeping from 1 kHz to 100 kHz with 10 frequencies/decade. To make measurements from sensors within grafts, de-ionised water and PBS were alternately flowed through the graft lumen using a VCS-6 gravity fed liquid perfusion system (Warner Instruments), and a time-series of impedance measurements was acquired.

Impedance measurements were performed from devices used in cell culture experiments using a Hioki IM3536 LCR meter (Hioki Corporation) controlled by LCR Meter Sample Application software (Hioki Corporation). The packaged sensors were again attached via a miniature FFC connector, with one electrode connected to the meter high side lead, and the other connected to the low side lead. Measurements were made using a 10 mV amplitude test signal, with a current limit of 10 μA, sweeping from 1 kHz to 1 MHz in 1 kHz intervals.

E. In vitro sensor characterization

Cultured VSMCs were used to create a realistic in vitro test-bench for the FCOF sensor. Primary cultures of mouse aorta smooth muscle cells, derived from a transgenic mouse model, were used as previously described [21]. They were grown in Dulbecco's Modified Eagle Medium (DMEM) supplemented with HEPES, 10% foetal bovine serum, penicillin, streptomycin, and L-glutamine (all from Gibco), and maintained in an incubator at 37˚C with a 5% CO_2 atmosphere. Packaged cell impedance sensor devices were sterilised in 70% ethanol and rinsed three times in sterile water prior to use. To obtain an initial control (no cells) measurement, each device was immersed in 3 ml of culture medium, and an impedance measurement was performed. They were then seeded with 2.5 × 10^5 cells/device and returned to the incubator for 24 h to allow cell adhesion and proliferation. Following this growth period, an optical microscope inspection was made, and the impedance measurement repeated.

For testing in blood, clotted and un-clotted (1mM EDTA) porcine blood was collected post-mortem, and 5 ml aliquots of each were prepared. Measurements were performed with the sensor in the centre of each sample. Sensors were cleaned between measurements using 70% ethanol and sterile water.

F. Graft Fabrication

We partnered with a commercial supplier of vascular devices (Zeus Industrial Products, Inc.) to produce a custom expanded polytetrafluoroethylene (ePTFE) graft. The production run was undertaken using a custom metal die to introduce sensor

channels within the graft wall. ePTFE was forced through the extrusion die to create graft material with an outer diameter of 10 mm and a large inner lumen with four circumferential smaller lumens. The inner lumen diameter was 6 mm, the circumferential channels had a cross sectional height of 0.5 mm and width of 3.2 mm to accommodate the FCOF package. The inner lumen and circumferential channels ran the full length of the graft material. Prior to integration with the FCOF package, the graft material was subjected to amorphous locking at approximately 800˚C.

G. Data Analysis

Data from lifetime testing and graft flow experiments were processed using MATLAB R2020b (MathWorks) to produce a time-series of impedance at specific frequencies. Microsoft Excel was used for all other data handling. Data from cell culture experiments were analysed using a two-way repeated measures ANOVA to test for the effects of frequency and cell growth or blood clotting on impedance. Statistical analysis and data plotting was performed using Prism 8 (GraphPad Software). All data in text and figures are presented as mean ± standard deviation.

III. Sensor Design & Fabrication

Dies carrying miniature platinum interdigitated electrode (IDE) arrays were microfabricated on silicon wafers Fig. 2(a). Each IDE contained 10 fingers, 25 μm wide and 500 μm long, with a pitch of 50 μm (leaving a 25 μm gap between each finger). This gave an overall sensitive region on each IDE of 500 μm × 475 μm. Similar electrode dimensions were previously reported to provide highly sensitive detection of VSMC using unpackaged bare IDEs in vitro [22]. Three identical and independent IDE arrays were placed on each die to provide redundancy during characterisation. Low resistance aluminium tracks were used for all on-die interconnect. To enable electrical and mechanical integration with the flexible substrate, rows of six aluminium bond pads (width 110 μm, pitch 210 μm) were positioned at each end of the die. One (connected) row provided an electrical link to the IDE electrodes, while the other (dummy) row ensured even bonding forces across the die, die/substrate co-planarity, and additional mechanical strength. Fiducial marks were also added at each corner to the die to enable optical alignment with the substrate during flip-chip bonding. The overall die size was 1.40 mm × 3.00 mm, with a thickness of 525 μm. While this is already sufficiently compact for implantable applications, we anticipate that future reductions in volume will be possible by decreasing the number of IDE arrays on each die, optimising the die floorplan, and using back-grinding techniques to thin the bulk silicon.

The flexible substrate was fabricated from polyimide with a single layer of copper track and a top layer of coverlay for electrical insulation (Fig. 2b). Local polyimide stiffeners were used to provide sufficient mechanical strength for flip-chip bonding. Six tracks (width 0.11 mm, pitch 0.21 mm) were fabricated in the copper layer to create substrate bond pads and connections to a miniature FFC connector (6 contacts, width 0.3 mm, pitch 0.5 mm). An additional unconnected substrate bond pad area was fabricated at the far end of the die attach area for bonding with dummy pads on the die. Optical alignment fiducials were included at each corner of the die attach area, complimentary to those on the die. A sensor window of 0.80 mm × 1.90 mm (W × L) in the centre of the die attach area provides sensor access to the external environment. The flexible substrate had overall dimensions of 2.0 mm × 100.0 mm (W × L), widening to 3.4 mm at the FFC connector.

The die and substrate were co-designed to create a low-profile FCOF package (Fig. 3a), suitable for integration with implantable vascular devices. The package was assembled using flip-chip bonding, with gold stud bumps on the die and thermosonic bonding for attachment to the substrate. Inspection of the assembly using microfocus radiography showed that the

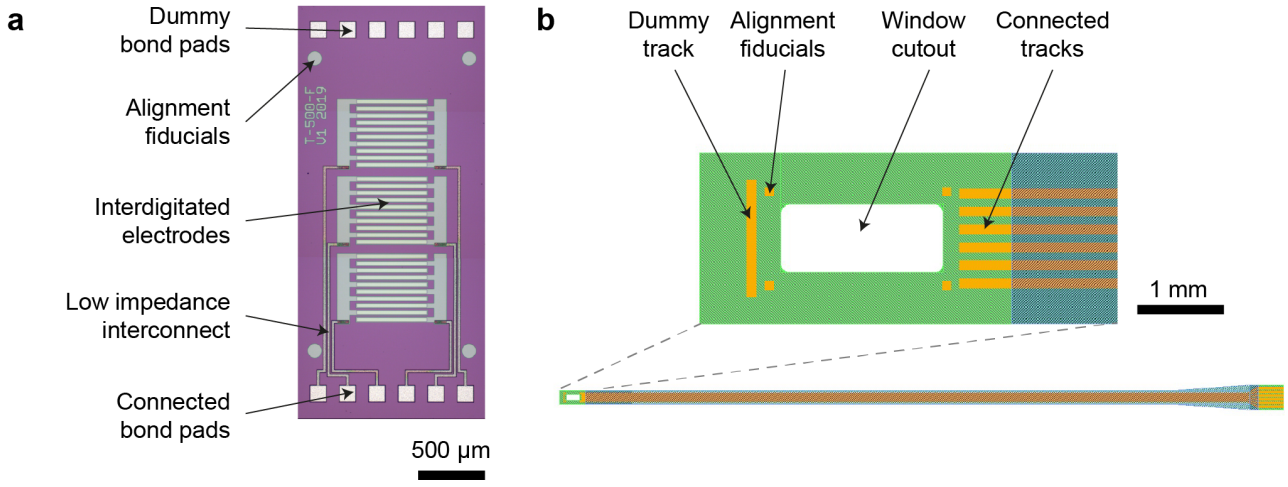

Fig. 2. Sensor die and flexible substrate co-design for flip-chip bonding. (a) Photograph showing the fabricated IDE die. (b) Schematic of the flexible substrate layout.

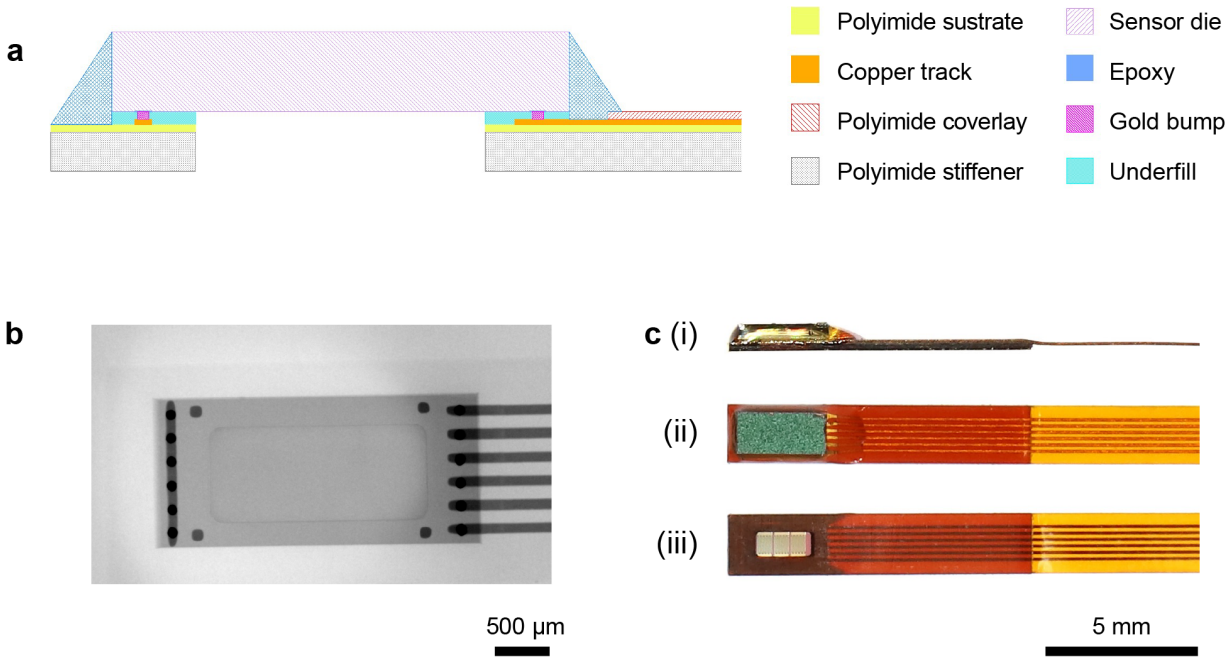

Fig. 3. Flip-chip assembly and moisture resistant packaging. (a) Schematic cross-section through the long axis of the sensor, showing bond positions, electrical insulation, and sensor window. (b) Microfocus radiograph showing assembled device after flip-chip bonding. (c) Photographs showing the completed FCOF package.

flip-chip optical alignment process was successful (Fig. 3b). A layer of underfill was applied to insulate and support the bonds, and epoxy was used to insulate the die edges and exposed copper tracks. The die backside was not covered with epoxy, as it was already insulated with a layer of silicon dioxide during fabrication. The finished sensor (including stiffener and die) was approximately 900 μm thick (Fig. 3c). This FCOF package successfully combines moisture resistance for the bond connections and selective exposure of the die surface. It is also sufficiently adaptable to host other sensors or electronic components (e.g., CMOS devices for analogue front-end and signal digitization). A wireless transmitter IC and antenna, necessary for a fully functional smart graft, may also be connected on the far end of the flex cable.

IV. Results & Discussion

A. Sensor characterization in solution

We initially tested the sensor performance in media with different conductivities to ensure that the IDE sensor was functional following assembly and packaging process. Impedance measurements were made in air (non-conductive), deionised water (low conductivity), and phosphate buffered 0.9% saline (PBS, high conductivity, equivalent to that of blood). We observed significantly higher impedance magnitudes in both air and water when compared to saline (Air: $1.49 \pm 0.13 \times 10^6$ Ω, Water: $1.22 \pm 0.03 \times 10^6$ Ω, PBS: $3.68 \pm 0.02 \times 10^3$ Ω; n = 3 sensors/condition, measured at 10 kHz), indicating that the IDE was correctly connected, and could

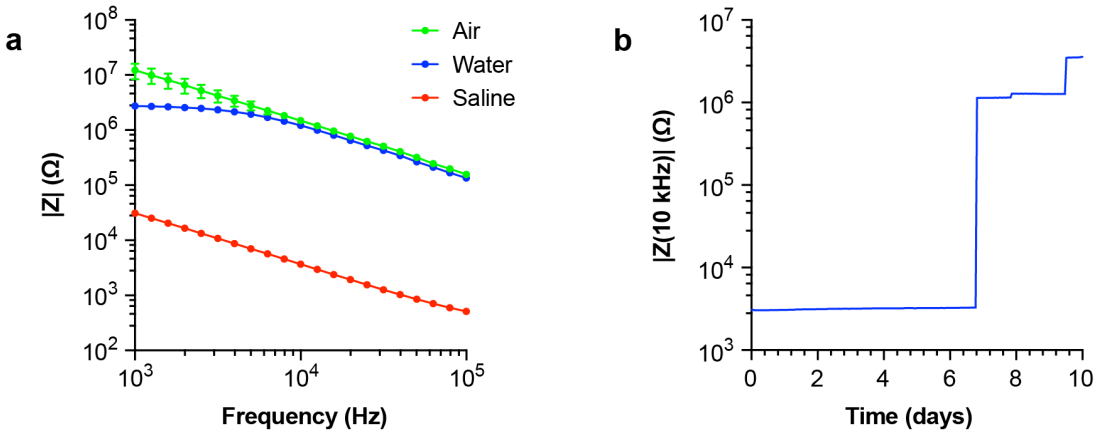

Fig. 4. Bench testing of packaged sensors. (a) Impedance spectroscopy of sensors in solution (n = 3 sensors/condition). (b) Example of a typical sensor failure, showing a rapid increase in impedance at the failure point.

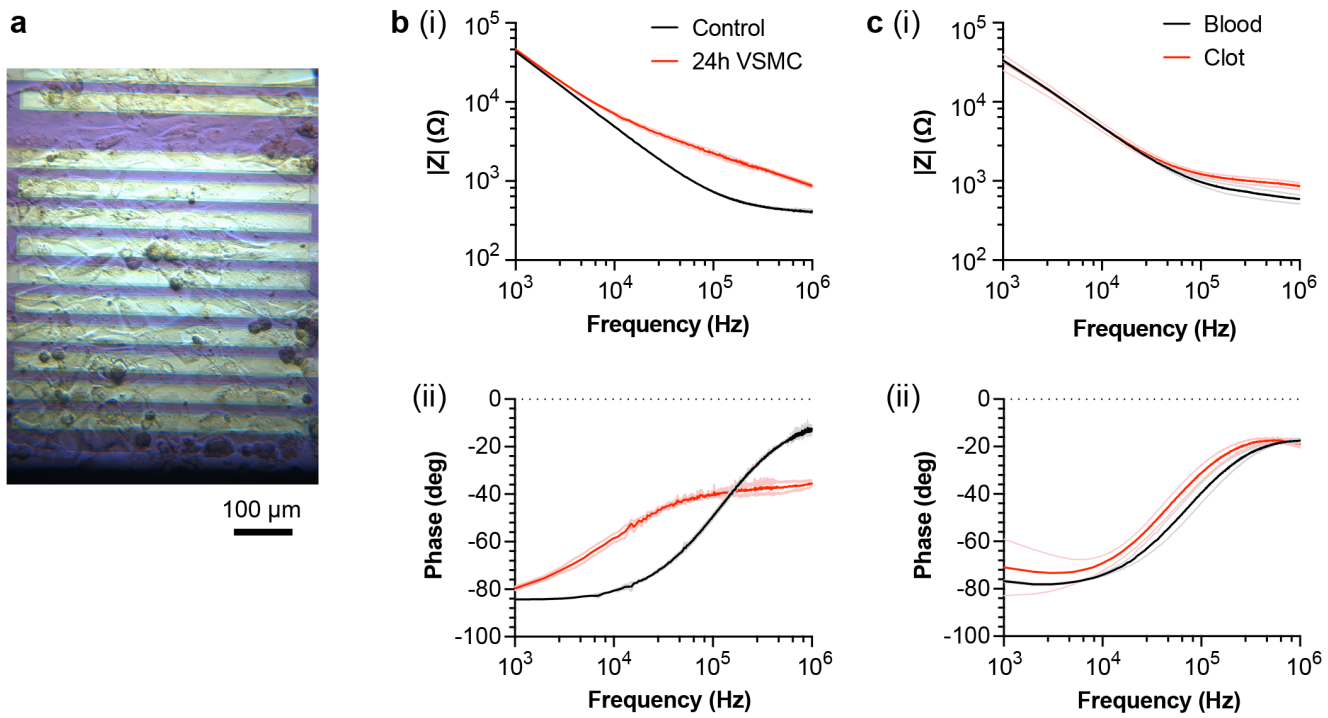

Fig. 5. In vitro biosensing performance assessment. (a) Microscope photograph of a monolayer of mouse aortic VSMC on the IDE surface of a packaged sensor, taken 24 h after seeding. (b) Impedance spectra measured before (control) or 24 h after seeding with VSMC, showing (i) magnitude, and (ii) phase (n = 3 repeats/condition; thick lines shows mean, light lines show SD). (c) Impedance spectra measured in the presence of unclotted or clotted blood, showing (i) magnitude, and (ii) phase (n = 3 repeats/condition; thick lines show mean, light lines show SD).

detect solution impedance effectively. The impedance also monotonically decreased with frequency (Fig. 4a), indicating the presence of interconnect and electrochemical double-layer capacitances in the system, as expected.

To estimate the package lifetime under simulated conditions of use, sensors were immersed continuously in PBS, and repeated measurements of the solution impedance were made. All sensors initially gave similar outputs. However, over time we eventually observed failures, evident as a rapid increase in impedance of several orders of magnitude (Fig. 4b), indicating a loss of connection between substrate and die. All sensors had a lifetime of ≥ 4.5 days (n = 3 sensors; two failed after 4.5 and 6.8 days, one remained functional after 30 days). While this lifetime was sufficient for initial characterisation work, it will need to be further improved before clinical application. An initial target will be the underfill layer moisture resistance, which is essential for preventing corrosion of bonds and their associated metallisation [23].

B. *In vitro detection of VSMC*

Sensor performance was next tested using primary cultures of mouse aortic VSMC as an in vitro model of neointimal hyperplasia [2]. Baseline (control) impedance measurements of cell culture medium using the packaged sensor gave results equivalent to those obtained in PBS, as expected. VSMC were then seeded on the sensor and grown for 24 h, allowing an adherent monolayer of cells to form on the electrode surfaces (Fig. 5a). Following this growth period, the impedance magnitude showed a significant increase compared to control measurements ($p < 0.0001$), corresponding to a reduced conductivity between IDE electrodes due to the presence of cells (Fig. 5b(i)). The impedance phase also showed a significant difference following the growth period ($p = 0.0003$). When compared to control measurements, VSMC caused a less negative phase shift at low frequencies (~10^4 Hz) and more negative shift at high frequencies (~10^6 Hz) (Fig. 5b(ii)).

These results are all consistent with previously reported electrical cell-substrate impedance sensing (ECIS) studies, which show that adherent cells cause a general increase in impedance magnitude, with the resistive component dominating at low frequencies (due to movement of charge in gaps between cells), and the capacitive component at high frequencies (due to the dielectric properties of cell membranes) [24]. Together, these data provide a proof-of-concept for detection of VSMC tissue growth using the FCOF packaged sensor.

C. *In vitro performance in blood*

Since the sensor is designed to operate within a vascular graft, we also tested the sensor performance directly in fresh blood, and in the presence of a blood clot (Fig. 5c). The measured blood impedance spectrum had a similar profile and slightly greater magnitude to that of cell culture medium. Presence of a clot on the sensor surface significantly increased the measured impedance ($p = 0.029$) and affected the phase ($p = 0.049$). These results show that the sensor performs effectively in blood and can successfully discriminate changes in this environment.

D. *Sensor integration with vascular graft*

Finally, we explored the mechanical integration of the packaged

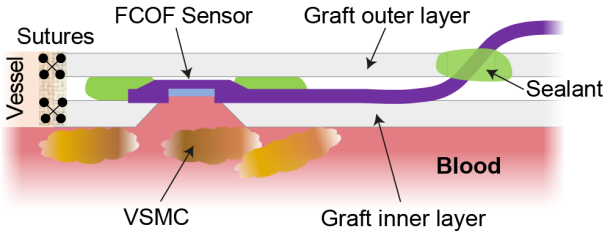

Fig. 6. Sensor integration with a PTFE vascular graft. Cross-section illustrating position of the packaged sensor within the graft.

sensor with a custom ePTFE vascular graft, frequently used for creating AV access fistulae in haemodialysis patients [25]. These grafts are typically implanted in a loop between the brachial artery and vein in the forearm (Fig. 1a). Since neointimal hyperplasia of VSMC that could lead to stenosis typically occurs close to the vessel/graft join site [8], the sensor should ideally be positioned close to this area. To integrate the sensor and graft, we developed a novel synthetic graft design consisting of an ePTFE tube with an additional narrow lumen to carry the sensor leads. A suitable window was also included in the inner surface, allowing sensor access to the lumen of the graft Fig. 6.

This design is highly manufacturable, physically robust, would minimize the risk of blood leakage in the case of sensor detachment, and creates a conduit for the lead that can be brought out to the graft surface at a convenient point to connect other electrical components and wireless interface. However, the sensor window inevitably introduces irregularities into the graft surface that may form nucleation points for unwanted VSMC growth [8]. Future *in vivo* testing, followed by detailed histopathological analysis of hyperplasia within the graft, would be required to investigate this effect.

A prototype of this design was fabricated to investigate feasibility of the concept (Fig. 7a,b). The sensor was positioned at the end of the graft, where it would be able to sense VSMC growth at the anastomosis. Four narrow lumens were included to enable future integration with multiple sensors, although here we only trialled integration of a single sensor. To test the functionality of the complete graft and sensor, we sequentially flowed liquids with different conductivities (water and PBS) through the main lumen of the graft and measured the solution impedance over time. This showed the expected changes in impedance as the solutions were exchanged (Fig. 7c), equivalent to those measured previously in static solutions (Fig. 4a). Together, this shows that the sensor was successfully integrated without damage and can accurately report changes within the graft environment in real-time.

E. Comparison with other vascular graft sensors

Existing vascular implant monitoring systems sense pressure to determine whether the graft has become occluded. These devices use piezoresistive [4], MEMS [5], or piezoelectric [6,7] pressure sensors. They have demonstrated effective detection of disrupted blood flow that is characteristic of late-stage occlusion, however they do not allow detection of the earliest signs of VSMC growth that would occur within the graft lumen, as described in this work. Typically, these pressure sensors are placed on the outside of the ePTFE graft [4, 6]. This simplifies

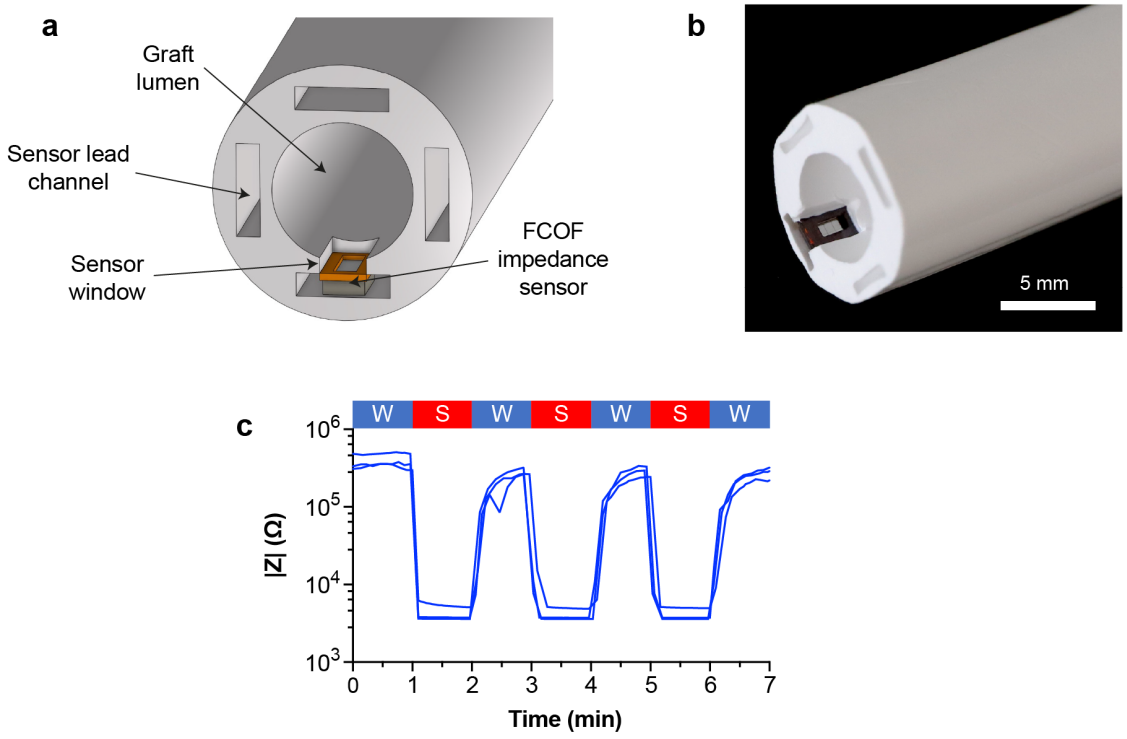

Fig. 7. Smart graft prototype. (a) Cross-section 3D rendering of the synthetic ePTFE graft and integrated FCOF impedance sensor; (b) photograph of the complete graft/sensor system. (c) Real-time sensing of impedance within the graft lumen, with repeated sequential changes of the flowing solution between deionised water (W) and PBS (S). Impedance was measured at 10 kHz (n = 3 sensors, shown as individual traces).

the graft design but prevents direct access to the lumen to enable early-stage detection of VSMC growth. Integration of graft pressure sensors with an application specific integrated circuit (ASIC) for wireless power and communications has also been demonstrated [5,7]. This suggests that the "smart graft" approach described here for our ECIS sensors is viable.

V. Conclusion

Implantation of vascular grafts is a routine procedure for various clinical conditions. However, grafts can trigger neointimal hyperplasia of VSMC at graft-vessel boundaries. We propose a novel sensor that could directly measure the increased cellular impedance caused by VSMC growth. This would enable direct measurement of the root cause of graft stenosis, in contrast to existing sensors that only measure blood-flow as a proxy for graft blockage. Real-time data from the sensor would provide a timely warning sign of graft failure, enabling earlier and more effective clinical interventions. The miniature prototype device was based on microsystem integration of a silicon-based sensor and a flexible substrate using FCOF assembly. We found that the packaged sensor could detect VSMC growth in vitro effectively. In addition, we demonstrated that the complete system could be integrated within the wall of a novel synthetic ePTFE graft and detect real-time changes in impedance. Our future work will focus on developing a new generation of silicon sensors that include high-precision integrated electronics situated close to the signal source, enabling autonomous sensing and transmission of graft condition.

Acknowledgement

We are grateful to Ewan Russell for his assistance with image preparation; Merlin Flex Ltd. for flexible PCB fabrication; Alter Technology for flip-chip bonding; and Zeus Industrial Products, Inc. for ePTFE graft manufacturing.

References

[1] M. K. Peck et al., "New Biological Solutions for Hemodialysis Access," *The Journal of Vascular Access*, vol. 12, no. 3, pp. 185-192, 2011, doi: 10.5301/jva.2011.6451.

[2] J. M. MacRae et al., "Arteriovenous Access Failure, Stenosis, and Thrombosis," *Canadian Journal of Kidney Health and Disease*, vol. 3, 2016, doi: 10.1177/2054358116669126.

[3] M. S. Conte et al., "Society for Vascular Surgery practice guidelines for atherosclerotic occlusive disease of the lower extremities: Management of asymptomatic disease and claudication," *Journal of Vascular Surgery*, vol. 61, no. 3, pp. 2S-41S.e1, 2015, doi: 10.1016/j.jvs.2014.12.009.

[4] H. Chong, J. Lou, K. M. Bogie, C. A. Zorman, and S. J. A. Majerus, "Vascular Pressure–Flow Measurement Using CB-PDMS Flexible Strain Sensor," *IEEE Transactions on Biomedical Circuits and Systems*, vol. 13, no. 6, pp. 1451-1461, 2019, doi: 10.1109/tbcas.2019.2946519.

[5] B. John et al., "A Stent Graft Occlusion Detection : Pressure Sensing Implant Device with Inductive Power and Data Telemetry," presented at the *2018 IEEE International Symposium on Circuits and Systems (ISCAS)*, 2018.

[6] R. F. Neville, S. K. Gupta, and D. J. Kuraguntla, "Initial in vitro and in vivo evaluation of a self-monitoring prosthetic bypass graft," *Journal of Vascular Surgery*, vol. 65, no. 6, pp. 1793-1801, 2017, doi: 10.1016/j.jvs.2016.06.114.

[7] J. H. Cheong et al., "An Inductively Powered Implantable Blood Flow Sensor Microsystem for Vascular Grafts," *IEEE Transactions on Biomedical Engineering*, vol. 59, no. 9, pp. 2466-2475, 2012, doi: 10.1109/tbme.2012.2203131.

[8] L. Li, C. M. Terry, Y.-T. E. Shiu, and A. K. Cheung, "Neointimal hyperplasia associated with synthetic hemodialysis grafts," *Kidney International*, vol. 74, no. 10, pp. 1247-1261, 2008, doi: 10.1038/ki.2008.318.

[9] I. Holland, C. McCormick, and P. Connolly, "Towards non-invasive characterisation of coronary stent re-endothelialisation – An in-vitro, electrical impedance study," *Plos One*, vol. 13, no. 11, 2018, doi: 10.1371/journal.pone.0206758.

[10] D. Rivas-Marchena, A. Olmo, J. Miguel, M. Martínez, G. Huertas, and A. Yúfera, "Real-Time Electrical Bioimpedance Characterization of Neointimal Tissue for Stent Applications," *Sensors*, vol. 17, no. 8, 2017, doi: 10.3390/s17081737.

[11] L. Shedden, S. Kennedy, R. Wadsworth, and P. Connolly, "Towards a self-reporting coronary artery stent—Measuring neointimal growth associated with in-stent restenosis using electrical impedance techniques," *Biosensors and Bioelectronics*, vol. 26, no. 2, pp. 661-666, 2010, doi: 10.1016/j.bios.2010.06.073.

[12] T. Süselbeck et al., "In vivo intravascular electric impedance spectroscopy using a new catheter with integrated microelectrodes," *Basic Research in Cardiology*, vol. 100, no. 1, pp. 28-34, 2004, doi: 10.1007/s00395-004-0501-8.

[13] D. D. Stupin et al., "Bioimpedance Spectroscopy: Basics and Applications," *ACS Biomaterials Science & Engineering*, vol. 7, no. 6, pp. 1962-1986, 2021, doi: 10.1021/acsbiomaterials.0c01570.

[14] Y. Xu, X. Xie, Y. Duan, L. Wang, Z. Cheng, and J. Cheng, "A review of impedance measurements of whole cells," *Biosensors and Bioelectronics*, vol. 77, pp. 824-836, 2016, doi: 10.1016/j.bios.2015.10.027.

[15] A. Tsiamis et al., "Comparison of Conventional and Maskless Lithographic Techniques for More than Moore Post-Processing of Foundry CMOS Chips," *Journal of Microelectromechanical Systems*, vol. 29, no. 5, pp. 1245-1252, 2020, doi: 10.1109/jmems.2020.3015964.

[16] J. Schmitz, "Adding functionality to microchips by wafer post-processing," *Nuclear Instruments and Methods in Physics Research Section A: Accelerators, Spectrometers, Detectors and Associated Equipment*, vol. 576, no. 1, pp. 142-149, 2007, doi: 10.1016/j.nima.2007.01.142.

[17] J. R. K. Marland et al., "Real-time measurement of tumour hypoxia using an implantable microfabricated oxygen sensor," *Sensing and Bio-Sensing Research*, vol. 30, 2020, doi: 10.1016/j.sbsr.2020.100375.

[18] E. Perfecto and K. Srivastava, "Technology Trends: Past, Present, and Future," in *Advanced Flip Chip Packaging*, 2013, ch. Chapter 2, pp. 23-52.

[19] S.-C. Kim and Y.-H. Kim, "Review paper: Flip chip bonding with anisotropic conductive film (ACF) and nonconductive adhesive (NCA)," *Current Applied Physics*, vol. 13, pp. S14-S25, 2013, doi: 10.1016/j.cap.2013.05.009.

[20] G. Dou and A. S. Holmes, "Thermosonic flip-chip assembly on flex substrates," presented at the *2012 13th International Thermal, Mechanical and Multi-Physics Simulation and Experiments in Microelectronics and Microsystems*, 2012.

[21] J. Mercer, N. Figg, V. Stoneman, D. Braganza, and M. R. Bennett, "Endogenous p53 Protects Vascular Smooth Muscle Cells From Apoptosis and Reduces Atherosclerosis in ApoE Knockout Mice," *Circulation Research*, vol. 96, no. 6, pp. 667-674, 2005, doi: 10.1161/01.RES.0000161069.15577.ca.

[22] A. Bussooa et al., "Impedimetric Detection and Electromediated Apoptosis of Vascular Smooth Muscle Using Microfabricated Biosensors for Diagnosis and Therapeutic Intervention in Cardiovascular Diseases," *Advanced Science*, vol. 7, no. 18, 2020, doi: 10.1002/advs.201902999.

[23] L. Bowman and J. D. Meindl, "The Packaging of Implantable Integrated Sensors," *IEEE Transactions on Biomedical Engineering*, vol. BME-33, no. 2, pp. 248-255, 1986, doi: 10.1109/tbme.1986.325807.

[24] J. A. Stolwijk, K. Matrougui, C. W. Renken, and M. Trebak, "Impedance analysis of GPCR-mediated changes in endothelial barrier function: overview and fundamental considerations for stable and reproducible measurements," *Pflügers Archiv - European Journal of Physiology*, vol. 467, no. 10, pp. 2193-2218, 2014, doi: 10.1007/s00424-014-1674-0.

[25] J. A. Akoh, "Prosthetic Arteriovenous Grafts for Hemodialysis," The *Journal of Vascular Access*, vol. 10, no. 3, pp. 137-147, 2018, doi: 10.1177/112972980901000301.